Design of the Heliospheric Imager for the STEREO mission

Jean-Marc Defise[a*], Jean-Philippe Halain[a], Emmanuel Mazy[a], Russel A. Howard[b], Clarence M. Korendyke[b], Pierre Rochus[a], George M. Simnett[c], Dennis G. Socker[b]*, David F. Webb[d]

[a]Centre Spatial de Liège, 4031 Angleur, Belgium
[b]Naval Research Laboratory, Washington, DC 20375
[c]University of Birmingham, Birmingham B15217, United Kingdom
[d]Boston College, Chestnut Hill, MA 02467

ABSTRACT

The Heliospheric Imager (HI) is part of the SECCHI suite of instruments on-board the two STEREO spacecrafts. The two HI instruments will provide stereographic image pairs of solar coronal plasma and address the observational problem of very faint coronal mass ejections (CME) over a wide field of view (~90°) ranging from 12 to 250 R_{-0}. The key element of the instrument design is to reject the solar disk light, with stray-light attenuation of the order of 10^{-12} to 10^{-15} in the camera systems. This attenuation is accomplished by a specific design of stray-light baffling system, and two separate observing cameras with complimentary FOV's cover the wide field of view. A multi-vane diffractive system has been theoretically optimized to achieve the lower requirement (10^{-13} for HI-1) and is combined with a secondary baffling system to reach the 10^{-15} rejection performance in the second camera system (HI-2).

This paper presents the design concept of the HI, and the preparation of verification tests that will demonstrate the instrument performances. The baffle design has been optimized according to accommodation constrains on the spacecraft, and the optics were studied to provide adequate light gathering power. Stray-light has been studied in the complete configuration, including the lens barrels and the focal plane assemblies. A specific testing facility is currently being studied to characterise the effective stray-light rejection of the HI baffling. An overview of the developments for those tests is presented.

Keywords: heliospheric imager, stray-light, baffling, rejection test

1. INTRODUCTION

The NASA Solar Terrestrial Relations Observatory (STEREO) mission will place two spacecraft into nearly circular solar orbits, in the ecliptic plane, and with radii ~1 astronomical unit (AU). One spacecraft will lead, and the other will lag, the earth's own 1 AU orbital path and both will separate from earth at an average rate of 22º/year over the 2-5 year mission life. The three-axis stabilized sun pointed spacecraft carry a suite of remote sensing and in situ experiments. On the Sun Earth Connection Coronal and Heliospheric Investigation (SECCHI) experiment, the Heliospheric Imager (HI) will cover the heliosphere out to the earth's orbit in white light. The HI filed of view will partially overlap the extended solar corona (COR-2) in order to provide stereographic image pairs of the volume of space extending from the sun to the earth. The complete SECCHI field of view also includes the lower solar corona, observed in extreme ultraviolet emission lines.

The most notable scientific questions to be investigated by SECCHI pertain to coronal mass ejections (CMEs). CMEs are a class of large-scale transient phenomena revealed most effectively in white light time-series observations of the corona. They are characterized by explosive and outwardly expanding coronal density fluctuations that escape the solar gravitational

* Correspondence:
- Email: socker@lambda.nrl.navy.mil; Telephone: 202-767-2093; Fax: 202-767-5636
- Email: jmdefise@ulg.ac.be; Telephone: +32 4 367 6668; Fax: +32 4 367 5613

potential well and propagate into the heliosphere. SECCHI is designed to identify the processes that initiate CMEs, determine their three-dimensional structure, measure their acceleration, study their interaction with the heliosphere and explore the details of their relationship to geomagnetic storms.

2. OBSERVATIONAL CONSIDERATIONS

The STEREO mission orbital configuration (figure 1) ensure an ideal stereoscopic imaging instrument for optical remote sensing observation of CMEs in the region of the heliosphere from 30 R_ to 215 R_ (earth orbit), with a nearly hemispherical sun centered field of view in this region of the heliosphere. The SECCHI/Heliospheric Imager (HI) described in this paper trades the very wide hemispheric field of view for a smaller field of view with superior sensitivity to the extremely faint and potentially geoeffective CMEs propagating within the heliospheric volume centered along the sun-earth line. It is designed to acquire a white light image data set suitable for stereographic reconstruction of CMEs propagating through the inner heliosphere near the sun-earth line from $12R_0$ to ~$215R_0$. Detection of the CME signal against the natural background is a strong function of elongation (ε) (figure 2). The CME signal strength profile[6] varies as R^{-2} to R^{-3} so the signal decreases about four orders of magnitude between the outer corona and ε = 90º. The sum of the electron corona and the dust corona (K+F) background brightness[7,8] varies as $R^{-2.25}$ to $R^{-2.47}$ so it decreases by about three orders of magnitude between the outer corona and ε = 90º. CME signal detection is background noise limited for all elongations, since the typical CME is ~1% of the natural background in the HI field of view. Additive instrumental backgrounds can further reduce sensitivity to the faint CME signal. Instrumental backgrounds due to stray photospheric light, cosmic rays incident on the solid state detector, improperly processed transverse stellar image motion, planets and earthshine (during the early part of the mission) are all potentially significant sources of instrumental background.

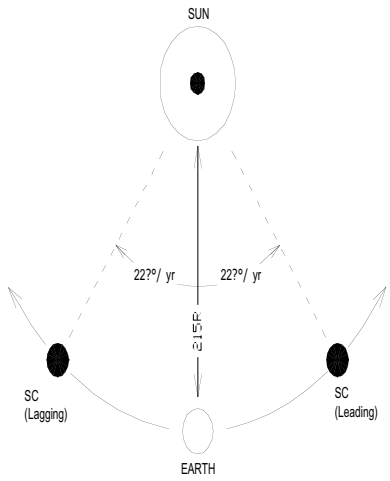

Figure 1. STEREO Mission orbit geometry
View from north ecliptic pole.

The most appropriate instrumentation for CME observation changes with CME signal detection conditions and is thus a strong function of elongation. At small elongation, the relatively bright signal, narrow required field of view, and strong photospheric and coronal backgrounds suggest an externally occulted coronagraph. On the other hand, at high elongation, the extremely low CME signal, wide required field of view, and faint night sky suggest a heavily baffled, high light gathering power (LGP), and wide-angle all-sky telescope. The HI accommodates these disparate requirements with two specialized camera systems (HI-1 & HI-2) in a nested and progressively baffled mechanical structure. Therefore, it provides the first opportunity to close the current ~185 R_0 wide geoeffective CME observation gap between the sun and the earth with high quality stereographic image pairs. It must be capable of detecting the extremely faint CME signal over a wide (~90°) field of

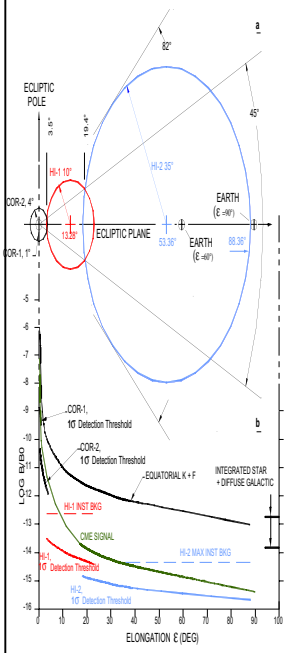

Figure 2. SECCHI fields of view and signal detection conditions

view, which approaches within a few degrees of the bright solar disk and includes the bright earth. In consequence, in the HI concept, rejection of the solar disk light is of paramount importance, since the natural object space background level (B) varies from 10^{-7}-10^{-14} of the brightness of the solar disk (B_0) and the CME signal is only 10^{-2} of the night sky at high elongation, or 10^{-16} B_0.

3. INSTRUMENT CONCEPT

The HI instrument shown in figure 3 is mounted on a side panel of the STEREO spacecraft whose normal is both in the ecliptic plane and perpendicular to the line of sight from the spacecraft to the sun. The roll angles of the two spacecraft differ by 180º so the panel normal on both the leading and the lagging spacecraft intersect the sun-earth line. HI is oriented on the panel so the optical axes of its two camera systems are in the ecliptic plane and intersect the sun-earth line.

The HI accommodates its requirements with two camera systems (HI-1 & HI-2), with overlapping field of view. Both camera will be active at very low light level, so in addition to forward and perimeter baffle, the internal baffle parts is very important… TBC

3.1 Baffle concept

The first stage of the HI baffle system is configured as a rectangle located in a plane containing the line of sight from the spacecraft to the inner most field point off solar limb. The sun-facing base of the rectangle is referred to as the linear forward baffle set while the top and two sides of the trapezoid are referred to as the perimeter baffle set. The part of the baffling system located under the rectangular plane, deeper in the HI box, is referred to as the internal baffle.

The HI baffle structure can thus be divided in three sub-systems, each having specific function:

- the forward baffle
- the perimeter baffle
- the internal baffle

3.1.1. Forward baffle

The function of the forward baffle set is to reject the solar disk, and to a lesser extent the inner corona, light from both the open interior of the rectangle and the perimeter baffle system. The degree of solar disk rejection afforded by the forward baffle was computed using Fresnel's second order approximation to the Fresnel-Kirchhoff diffraction integral for a semi-infinite half-screen[10].

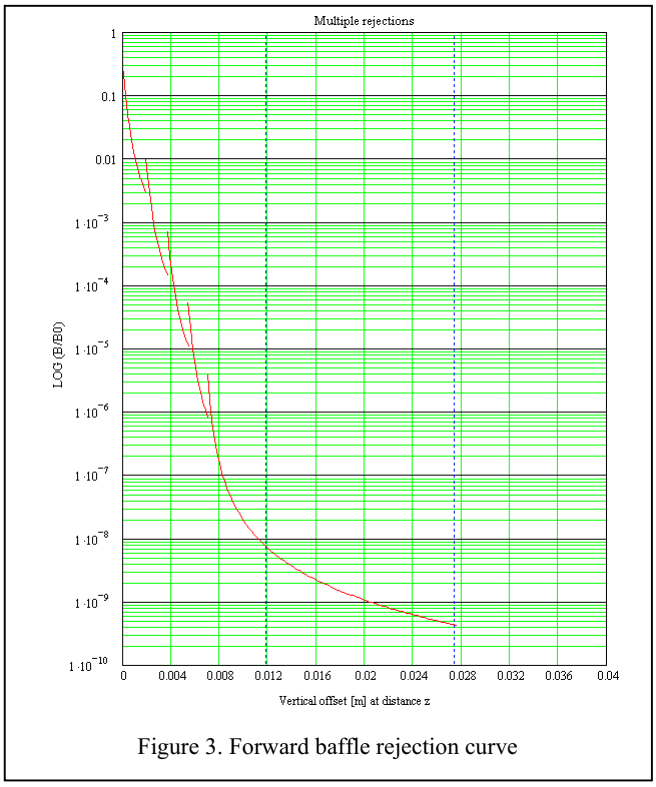

Figure 3. Forward baffle rejection curve

In the multi-vane approach, the vane edges are arranged in an arc such that the nth intermediate vane blocks the bright linear diffracting edge of the n-1 vane from the view of the n+1 vane edge. Fresnel's approximation can be applied to this arrangement as a cascade. The multi-vane design of the HI forward baffle is based on both laboratory tested baffle system for a similar heliospheric imaging experiment[11] and Fresnel computation. The Fresnel cascading rejection curve for the optimised forward baffle is shown on figure 3. The rejection level is < 3.10^{-8} B/B_0. With a 10^{-4} rejection factor at entrance aperture the rejection level is lower than 3.10^{-13} B/B_0.

Forward baffle thus protects HI-1 from sun disk brightness. The heights of the five linear edges of this baffle are arranged along a curve whose tangents at the first and the last vanes intersect the solar limb and the top edge of the HI-1 lens aperture respectively, the angle between these two tangents is referred to as the diffraction angle. The last vane of the forward linear

baffle system is the only edge visible to the HI-1 lens. It is imaged by the lens near a matching linear internal occulter coated with a highly absorbing material. The image plane of the external occulter is also slightly behind the internal occulter and the CCD front surface. However, since the distance from the last forward baffle vane to the lens is much greater than the focal length of the lens, the external occulter defocus at the internal occulter is minimal. HI-1 is therefore similar to an externally occulted coronagraph but without either a Lyot stop or a Lyot spot. Diffraction measurements[11,12] and Fresnel diffraction integral computations[10], with the forward baffle vane height distribution optimized for the HI-1 lens, ensure an instrumental background lower than 3.10^{-13} B/B_0 at the inner field cut off, $\varepsilon = 3.65°$ (13.67 R_0), will be achieved. This is below the natural K+F corona background in the small elongation bright sky regime and a factor of 10 better than the $<10^{-12}$ B/B_0 achieved on SOHO LASCO/C3[13]. The improvement over LASCO/C3 is due primarily to the substantially greater HI-1 inner field of view cut-off (13.67 R_0 vs. 3.8 R_0) and the fact that the Fresnel diffraction pattern intensity varies approximately with the inverse square of the diffraction angle.

3.1.2. Perimeter baffle

The main function of the three-sided perimeter baffle (two lateral and one rear parts) set is to protect the interior of the baffle system from solar photospheric light reflected or scattered from elements of the spacecraft located under its level.

3.1.3. Internal baffle

All spacecraft elements, with one exception, are required to remain below the extension of the trapezoidal baffle plane. The one exception is a single six meter long monopole antenna, one of the three nearly orthogonal monopoles deployed by the STEREO/WAVES (SWAVES) experiment low frequency radio receiver. Calculations and ray-tracing simulations indicate that scattered photospheric light from this monopole, which is directly illuminated by the solar photosphere, will be adequately trapped by the internal part of the HI baffle system.

The internal system thus contains a system of 9 tilted vanes to catch unwanted light (via multi-reflection, not diffraction) coming from SWAVES boom, together with light from planets, stars and zodiacal part of the sky. In addition to this system, a small vane above HI-1 and a group of two small vanes between HI-1 and HI-2 are part of the internal baffle.

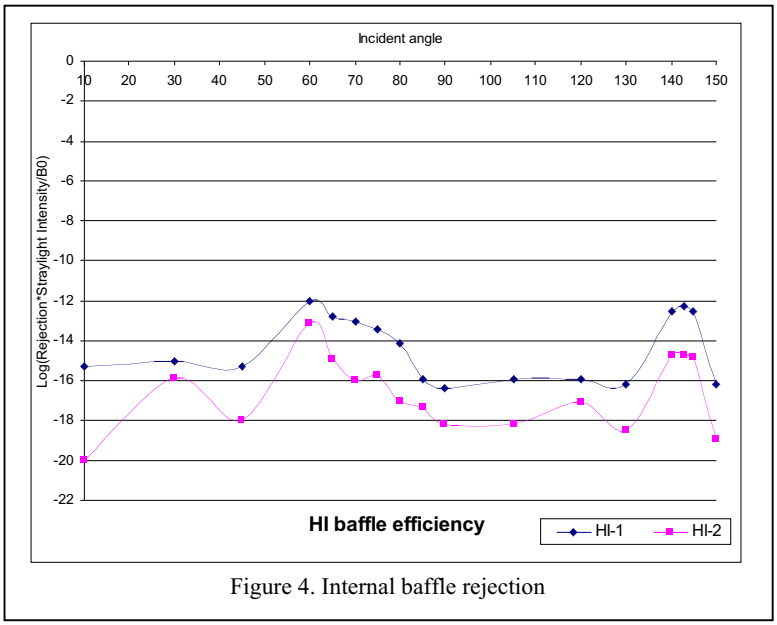

Figure 4. Internal baffle rejection

The inter-camera vanes system between the HI-1 and HI-2 apertures is designed to block light incident on the HI-1 camera face and its earthshine vane from scattering into the HI-2 entrance aperture. The small vane over the top of the HI-1 objective lens protects it from Earthshine. To avoid secondary straylight perturbations, it is located sufficiently deep in the forward baffle shadow. This location also results from a trade off between vignetting and overlapping of HI-1 and COR-2 field of view. Consequently, to ensure a 1 R_0 overlap between these two field of view, this small vane will partially vignette the upper part of the field of view, introducing a 0.9% lost light gathering power in the bottom part of the CCD.

Figure 4 shows the rejection level of the 9 vanes system for straylight sources located above the perimeter baffle, computed using ASAP™ ray-tracing software. Whatever the source orientation, the baffle rejection is $< 10^{-12}$. Considering again a 10-4 rejection at aperture stop, it guarantees a 10^{-16} rejection level at both HI-1 and HI-2 focal plane.

3.2 Camera design

The HI-1 camera utilizes a 20º field angle camera, slightly vignetted at its upper bound, centered 13.65º (~51 R_0) from the solar disk, a 2048x2048 pixel format CCD. The HI-2 camera consists of a 70° full field angle objective, i.e. a wide-angle fisheye lens, and a 2048x2048 pixel format CCD. The field angle compromise results in an effective LGP aperture diameter of about 7 mm on-axis. The HI-2 camera is set deeper within the forward baffle set shadow at a diffraction angle of 16.5º (upper solar limb to lens top edge), where the HI-1 forward baffle Fresnel diffraction calculation result is 10^{-15} B/B_0, well below the required 10^{-14} B/B_0. The HI-2 camera uses a second stage forward baffle matching internal occulter-stop located at the focal plane. The HI-2 instrumental background is dominated by veiling glare from earthshine diffracted at the objective aperture stop rather than baffle diffracted solar light. The instrumental background is $5x10^{-15}$ B/B_0 for a spacecraft-earth lead (lag) angle of 2º and thereafter diminishes approximately as the inverse square of the spacecraft-earth distance. Table 1 summaries the HI-1 and HI-2 camera characteristics, and figure 5 shows the HI-1 and HI-2 lens design.

	HI-1	**HI-2**
Field of View		
Half angle	10º	35º
Center	51.12R (13.65º)	200R (53.36º)
Inner Cutoff (Unvignetted)	13.67R (3.65º)	72.8R (18.36º)
Outer Cutoff (Unvignetted)	88.58R (23.65º)	332R (88.36º)
CCD Format	2048 x 2048 x 13.5_	2048 x 2048 x 13.5_
Plate scale	35.15”/pixel	2.05’/pixel
Objective	AR coated	AR coated
Diameter	16.0 (16) mm	20.7 (7.01) mm
Focal length	78.4 mm	19.74 mm
F-ratio	f/4.9	f/2.8
Passband	6500 _ - 7500 _	4000 _ - 10000 _
Instrumental background	$<3x10^{-13}$ B/B_0	$<5x10^{-15}$ B/B_0
Nominal exposure time	12 sec	60 sec
SNR	$\geq 30/(\text{pixel}\bullet\text{hr})^{1/2}$	$\geq 15.5/(\text{pixel}\bullet\text{hr})^{1/2}$

Table 1. HI instrument characteristics

Lens design of both HI-1 and HI-2 was realised using Synopsis™ and ASAP™ software. Light gathering, aberrations, defocus … were taken into account… TBC

…

…

…

…

…

…

…

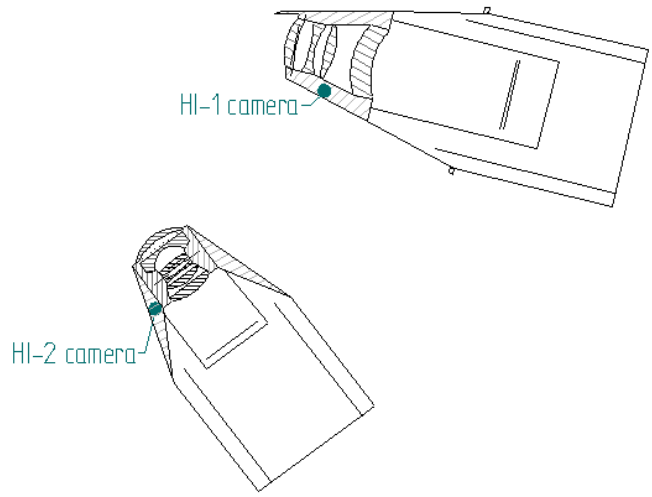

Figure 5. HI-1 and HI-2 lens design

In summary, the second camera aperture at a large diffraction angle, with additional staged baffling and a 70º wide angle lens will mitigate stray light rejection risk, improve threshold background noise limited signal detection at high elongation, and reduce the required overall dimensions of the perimeter baffle. The superior diffraction angle afforded the night sky portion of the field in this design is important since solar stray light rejection is the paramount risk. This approach to technical risk mitigation was driven by the fact that the empirically determined baffle diffraction performance has not been tested before below about 10^{-8} for wide-angle type diffraction baffle systems[11]. However Fresnel diffraction calculations indicate that the solar disk driven instrumental background of HI is below the natural object space background for all elongations within the respective fields of view (figure 3). This performance will be verified during straylight test as detailed in the following section.

4. DIFFRACTION TESTING

A complete testing facility is currently developed at CSL for stray-light verification of the HI forward baffle system. This test preparation is here presented in details. The stray-light test will assess Fresnel computations realised for one vane and for five vanes. In addition, an optimisation of the inter-vane separation is intended.

4.1 Test set-up

Figure 6 shows the conceptual configurations of the straylight test. In the first case, a photomultiplier will points toward the last vane edge and measure the rejection level at various angles. In the second case, the photomultiplier will be adapted to match with HI-1 field of view and then simulate incoming straylight in HI-1.

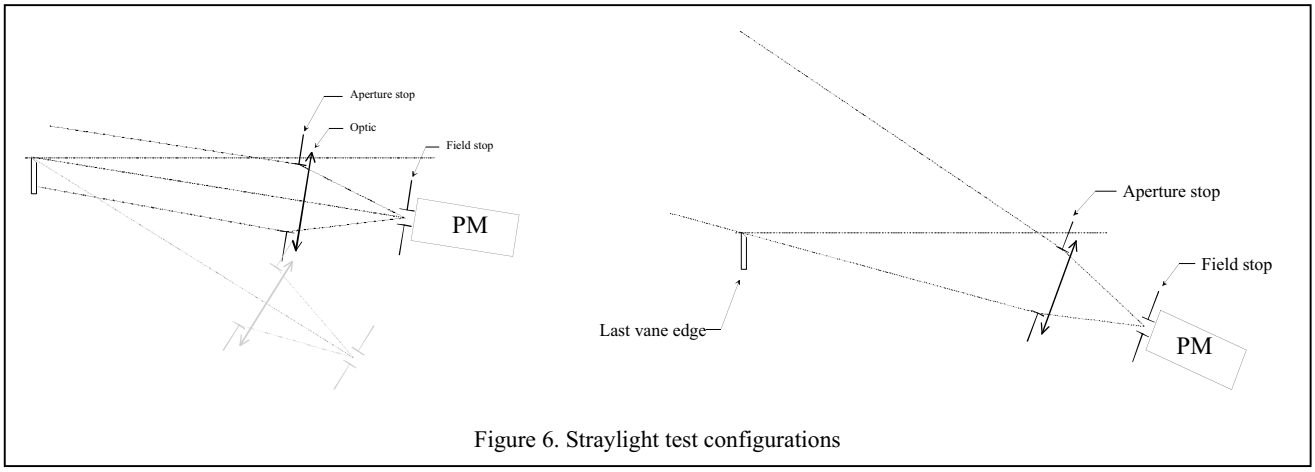

Figure 6. Straylight test configurations

To avoid particle diffusion that previously limited stray-light tests[11], the test will be performed in a vacuum chamber. Within such chamber, the Optical Ground Support Equipment (OGSE) will be confined in black shrouds to avoid any unwanted light and ensure black background.

Simulation of the sun brightness will be realised using a powerful laser source at 808nm (20 CW with a 600µm optic fiber), close to the HI-1 wavelength range. Specially design cooling system (-20°C) and HT power supply (1500V) has been developed, together with an attenuator in order to control the laser output. Link between laser and OGSE is realised using an optical fiber entering the vacuum chamber via a bridle with SMA905 connectors. Within the chamber, black shrouds and light-traps (attenuation of 10^{-9}) were designed to catch unwanted light and ensure perfect black environment around the photomultiplier. In addition, a collimator was designed to limit divergence of the optical fiber outcoming beam, and direct the beam onto the first vane edge of the mock up. This first vane is tilted to direct reflected light into a light trap and let only half of the beam being diffracted by the baffle. The mock-up is build to be as close as possible of the HI-1 configurations. Alignment of this OGSE will be realised using a 633nm He-Ne laser and specific theodolite configuration. Figure 7 shows the complete stray-light test set-up with its elements

4.2 Test plan

A first set of measurement will be realised to compare one vane rejection level with theoretical Fresnel calculations. Such comparison requires to measure diffracted light at various incident angles. Table 2 and Figure 8 summary expected rejection level for one vane (according to Fresnel theory).

CCD offset at 0.5m [mm]	Rejection level
10	10^{-4}
20	$1.5\ 10^{-5}$
30	$5\ 10^{-6}$

Table 2. One vane diffraction

A second set of measurement will then be realised to measure rejection level of five vanes. Table 3 and Figure 3 give the expected rejection level for five vanes according to Fresnel theory, with 20mm for inter-vane separation.

CCD offset at 0.5m [mm]	Rejection level
1.52	$4\ 10^{-3}$
3.02	$1.6\ 10^{-4}$
4.39	$7.5\ 10^{-6}$
5.64	$3.4\ 10^{-7}$
27.72	$4.7\ 10^{-11}$

Table 3. Five vane diffraction

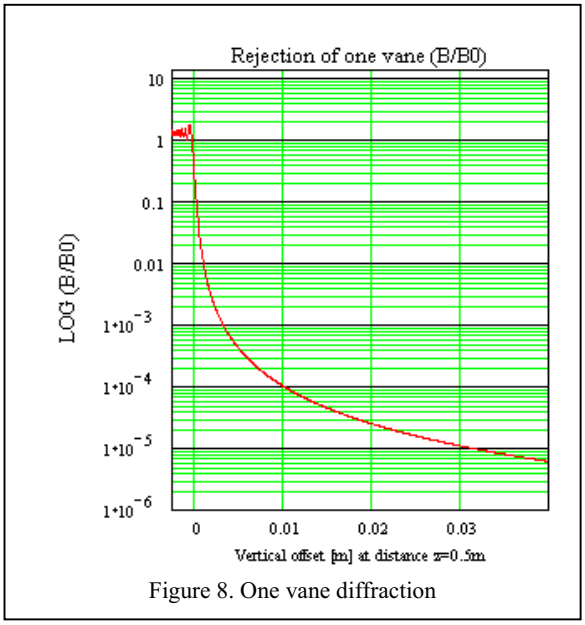

Figure 8. One vane diffraction

ACKNOWLEDGEMENTS

STEREO/SECCHI/HI is funded under NASA contract S-13631-Y.

REFERENCES

1. R.A. Howard, G.E. Brueckner, O.C. St.Cyr, D.A. Biesecker, K.P. Dere, M.J. Koomen, C.M. Korendyke, P.L. Lamy, A. Llebaria, M.V. Bout, D.J. Michels, J.D. Moses, S.E. Paswaters, S.P. Plunckett, R. Schween, G.M. Simnett, D.G. Socker, S.J. Tappin, D. Wang, "Observations of CMEs from SOHO/LASCO," *Coronal Mass Ejections*, N. Crooker, J.A. Joselyn, J. Freeman, editors, The American Geophysical Union, pp. 17-26, 1997.
2. A.J. Hundhausen, "An Introduction," *Coronal Mass Ejections*, N. Crooker, J.A. Joselyn, J. Freeman, editors, The American Geophysical Union, pp. 1-7, 1997.
3. C. Leinert and D. Kluppelberg, "Stray Light Suppression in Optical Space Experiments," *Applied Optics*, **13**, pp. 556-564, 1974.
4. I. Richter, C. Leinert, and B. Planc, "Search for Short Term Variations of Zodiacal Light and Optical detection of Interplanetary Plasma Clouds," *Astronomy and Astrophysics*, **110**, pp. 115-120, 1982.
5. D.F. Webb and B. V. Jackson, "The Identification and Characteristics of Solar Mass Ejections Observed in the Heliosphere by the Helios 2 Photometers," *Journal of Geophysical Research*, **95**, pp. 20641-20661, 1990.
6. B.V. Jackson, A. Buffington, P.L. Hick, S.W. Kahler, R.C. Altrock, R.E. Gold, and D.F. Webb, "The Solar Mass Ejection Imager", in *Solar Wind Eight*, D. Winterhalter, J. T. Gosling, S. R. Habal, W. S. Kurth, and M. Neugebauer, eds., AIP Conf. Proc. **382**, pp. 536-539, 1996.
7. S. Koutchmy and P.L. Lamy, " The F-corona and the circum-solar dust evidences and properties," in "Properties and Interactions of the Interplanetary Dust," IAU Colloq. **85**, pp. 63-74, 1985.

8. C. Leinert, I. Richter, E. Pitz, and B. Planck, "The Zodiacal Light from 1.0 to 0.3 A.U. as Observed by the Helios Space Probes," *Astronomy and Astrophysics*, **103**, pp. 177-188, 1981.
9. A. Buffington, "Very-wide-angle optical systems suitable for spaceborne photometric measurements," *Applied Optics*, **37**, pp. 4284-4293, 1998.
10. M. Born and E. Wolf, *Principles of Optics*, 6th (corrected) edition, Pergamon Press, New York, 1980.
11. Buffington, A. Jackson, B.V. and Korendyke, C.M., "Wide-angle stray-light reduction for a spaceborne optical hemispherical imager," *Applied Optics*, **35**, No. 34, pp. 6669-6673, 1996.
12. M. Romoli, H. Weiser, L.D. Gardner and J.L. Kohl, "Stray light suppression in a reflecting white light coronagraph," *Applied Optics*, **32**, pp 3559-3569, 1993.
13. G.E. Brueckner, R.A. Howard, M.J. Koomen, C.M. Korendyke, D.J. Michels, J.D. Moses, D.G. Socker, K.P. Dere, P.L. Lamy, A. Llebaria, M.V. Bout, R. Schwenn, G.M. Simnett, D.K. Bedford, C.J. Eyles, "The Large angle spectroscopic coronagraph (LASCO)," *Solar Physics*, **162**, pp. 357-402, 1995.
14. C.W. Allen, *Astrophysical Quantities*, 3rd edition, The Athlone Press, London, 1976.
15. A. Rose, "The Sensitivity Performance of the Human Eye on an Absolute Scale," *Journal of the Optical Society of America,* **38**, No. 2, pp. 196-208, 1948.
16. H.H. Barrett, "Objective assessment of image quality: effects of quantum noise and object variability," *Journal of the Optical Society of America*, A., **7**, No. 7, pp. 1266-1278, 1990.
17. A. Rose, "Quantum and Noise Limitations of the Visual Process," *Journal of the Optical Society of America*, **43**, No. 9, pp. 715-716, 1953.
18. D.G. Socker, R.A. Howard, C.M. Korendyke, G.M. Simnett, D.F. Webb, "The NASA Solar Terrestrial Relations Observatory (STEREO) Mission Heliospheric Imager", *SPIE* …